PERGAMON

Electrochimica Acta 44 (1999) 3283–3293

ELECTROCHIMICA Acta

Electrocatalysis of CO tolerance in hydrogen oxidation reaction in PEM fuel cells

S.J. Lee, S. Mukerjee, E.A. Ticianelli, J. McBreen*

Department of Applied Science, Brookhaven National Laboratory, Upton, NY 11973, USA

Received 3 July 1998; received in revised form 4 January 1999

Abstract

The electrocatalysis of CO tolerance in the hydrogen oxidation reaction was investigated for Pt/C, PtSn/C and PtRu/C electrocatalysts in proton exchange membrane (PEM) fuel cells. Both half and single cell polarization characteristics were studied at several temperatures and CO partial pressures. It is proposed that the CO adsorption step occurs predominantly through a displacement path for PtSn/C and through a free site attack path for CO on both Pt/C and PtRu/C. The data are more consistent with the participation of linear (PtSn/C, and PtRu/C [$T \leq 55^{\circ}C$]) and bridged bonded adsorbed CO on Pt/C and PtRu/C [$T \geq 70^{\circ}C$]. The CO oxidation process occurs at different potentials depending on the nature of the electrode material. The oxidation of CO by the alloy catalysts is not the only contributor to CO tolerance. Changes in the thermodynamics and the kinetics of the CO adsorption process, induced by the alloy catalysts, also contribute to CO tolerance.

Keywords: PEM fuel cells; CO tolerance; Hydrogen oxidation; CO oxidation; Electrocatalysis

1. Introduction

Gas diffusion electrodes with a loading of 0.1–0.2 mg cm^{-2} of dispersed platinum on carbon show very small polarization losses with respect of hydrogen oxidation in proton exchange membrane (PEM) fuel cells, when operating on pure H_2, but the losses are raised to unacceptable values when small amounts of CO are present in the fuel stream. On smooth bulk alloy electrodes, it has been found that presence of a second element with Pt such as Ru, Sn, Os, Mo, etc. either alloyed or as a codeposit, yields significant improvement in the CO tolerance relative to pure Pt [1–9]. In these cases, attempts to understand the mechanism of CO poisoning have focused on a variety experimental approaches, including the use of electrochemical techniques, in situ uv–visible and infrared reflectance spectroscopy, etc. [4,7,10–14].

Although these studies provide valuable information for the design of new catalysts, extrapolations of the conclusions with respect to the CO tolerance to the real systems are not straightforward, mainly because of use of reaction conditions different from the actual PEM fuel cell operating environment. Attempts to quantify the CO poisoning effect have been also made using phosphoric acid [15,16] and PEM [17–19] half and single cells, simulating as close as possible, the real conditions of a fuel cell. For the PEM system, some information regarding the kinetics and mechanism of the

* Corresponding author. Tel.: +1-516-344-4513; fax: +1-516-344-4071.

E-mail address: jmcbreen@bnl.gov (J. McBreen)

0013-4686/99/$ - see front matter
PII: S0013-4686(99)00052-3

reactions have been obtained by using different models for the processes taking place at the electrode [19,20]. Bellows et al. [20] have developed a CO_x inventory model for describing the behavior of adsorbed CO on Pt electrocatalysts, for a hydrogen feed containing CO and CO_2. One important conclusion of this work is that, under PEM fuel cell operating conditions, CO tolerance is achieved when the flux for CO electrooxidation balances the combined adsorption fluxes from both CO and CO_2. More recently, based on a simple kinetic model, Springer et al. [19] have shown that the polarization of the hydrogen electrode at low current density is limited essentially by the maximum rate of hydrogen dissociative chemisorption on a small fraction of the catalyst surface free of CO. It was also found that a rate of CO oxidation as low as 10 nA cm^{-2} (Pt) could have a significant effect in lowering the CO steady-state coverage and thus in increasing the magnitude of the hydrogen electrooxidation current.

This investigation examines both half and single cell polarization characteristics of CO tolerance of PtRu/C and PtSn/C relative to Pt/C in hydrogen oxidation reaction (HOR) in PEM fuel cells at several temperatures and CO partial pressures. In addition, the time response of the CO poisoning effects at several CO partial pressures as a function of cell potential and temperature has been studied.

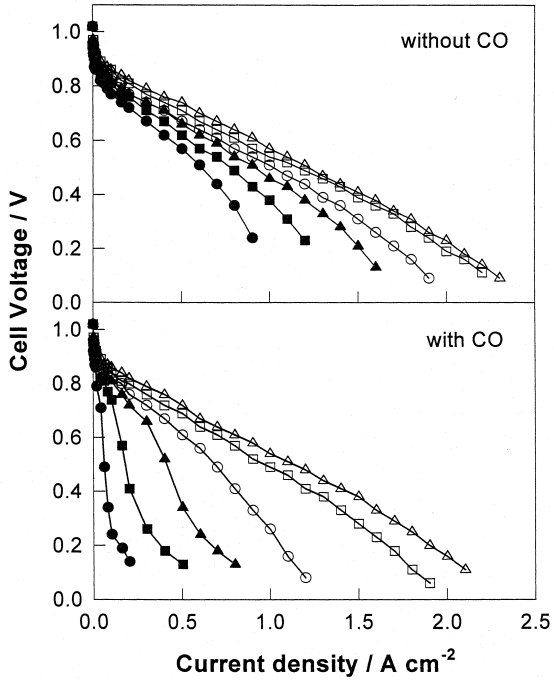

Fig. 1. Single cell performance plots for a Pt/C electrode with and without CO (20 ppm) at several temperatures: (●) 40°C; (■) 55°C; (▲) 70°C; (m) 85°C; (○) 100°C and (△) 115°C.

2. Experimental

Anode electrodes were prepared using catalyst powders (20 wt% Pt, PtRu (a/o 1:1) and PtSn (a/o 3:1) supported on Vulcan XC-72 carbon) purchased from E-TEK Inc (Natick, MA). The electrodes were made by a brushing/rolling technique with a total catalyst loading of approximately 0.4 mg/cm^2. The cathodes were commercial electrodes from E-TEK Inc. containing 0.4 mg/cm^2 platinum (20 wt% Pt on Vulcan XC-72). All the electrodes were impregnated with 1.9 mg/cm^2 (dry amount basis) of Nafion (Aldrich Chemical Co.). Nafion 115 membranes (DuPont, Fayetteville, PA) were used after cleaning in boiling 3% H_2O_2, 1 M H_2SO_4 and deionized water to remove organic and metallic impurities. The membrane and electrode assemblies (m and e) (5 cm^2) were prepared by hot pressing the electrodes onto the membrane at 140°C, 1000 kg_f/cm^2 for 3 min.

Steady-state polarization studies were conducted in a test cell which allowed simultaneous half and single cell polarization measurements. This was possible using a reversible hydrogen reference electrode on the anode side of the bipolar plate. The fuel cell test station, built in house, had arrangements to control, gas flow rate (mass flow controller, Matheson model 8247), cell temperatures, humidification and pressure. The performance evaluation of the single cells was carried out using a personal computer controlled electronic load (HP-6050A, Hewlett Packard Co.) interfaced through a GPIB board. Reactant gas pressures were adjusted at each temperature in order to keep a constant pressure of 1 atmosphere for the partial pressure of hydrogen and oxygen in the water vapor mixtures.

The single/half cell polarization data in the absence of CO were obtained prior to the experiments in the presence of the catalyst poison. The first measurements after switching to H_2/CO mixtures involved current vs. time response at a constant cell potential (typically 0.6 V). These data were recorded at several temperatures, CO concentrations and cell potentials, until the variation of the current with time was smaller than 200 μA cm^{-2} min^{-1}. Thereafter, the polarization data in the presence of CO were measured. Finally, in order to completely remove CO from the poisoned catalyst, the CO mixed gas was switched back to pure H_2 gas with the electrode polarized at 0.6 V for 2 h prior to any other measurements. Complete removal of CO was confirmed by comparing H_2/O_2 polarization data with corresponding data from electrodes never exposed to CO.

Measurements were conducted using H_2/O_2 and H_2–

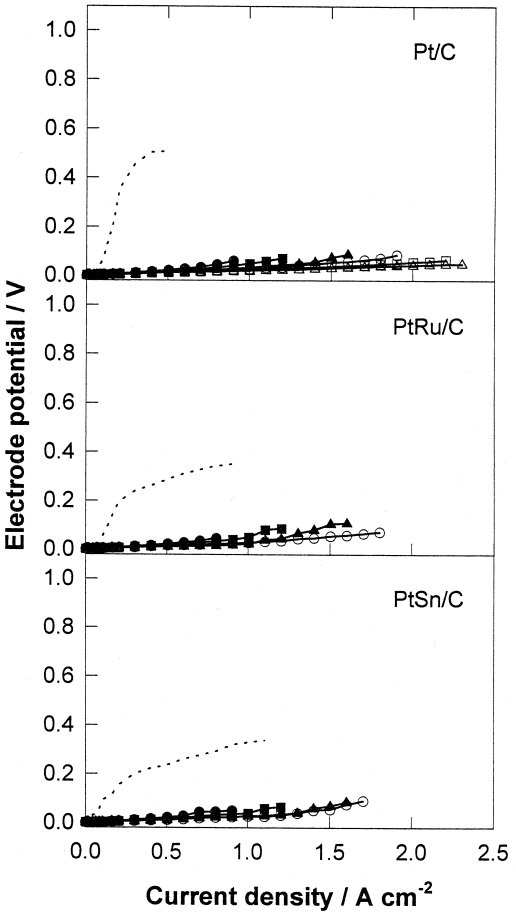

Fig. 2. Polarization of the hydrogen electrode for Pt/C, PtRu/C and PtSn/C without CO at several temperatures: (●) 40°C; (■) 55°C; (▲) 70°C; (○) 85°C; (□) 100°C; (△) 115°C and with CO at 55°C (· · ·).

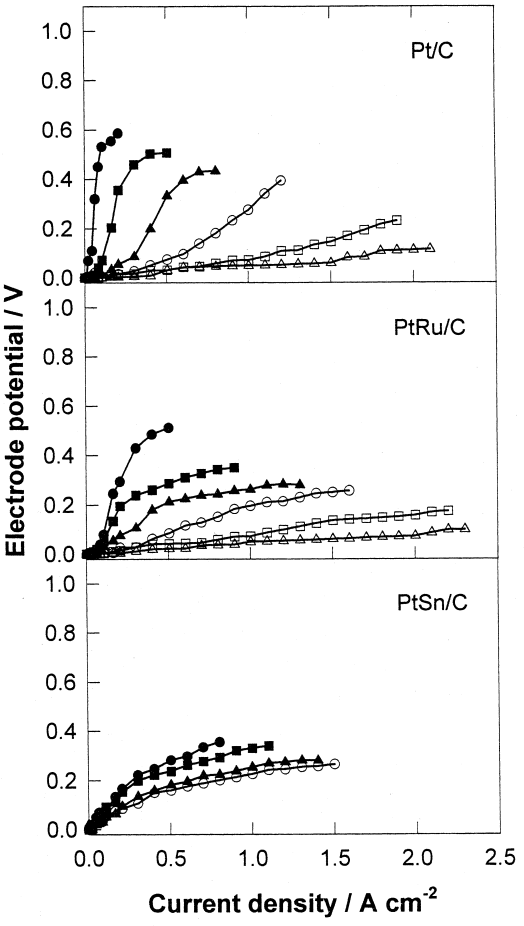

Fig. 3. Polarization of the hydrogen electrode for Pt/C, PtRu/C and PtSn/C with 20 ppm CO at several temperatures: (●) 40°C; (■) 55°C; (▲) 70°C; (○) 85°C; (□) 100°C and (△) 115°C.

CO/O_2 over a temperature range of 40–115°C. CO tolerance was measured in the concentration range of H_2/CO from 5 to 100 ppm. Polarization of the anode electrodes in presence of CO (E_{H_2+CO}) as a function of current density was obtained from measurements of the hydrogen electrode polarization (E_{H_2}) without CO, measured with respect to the RHE reference electrode, and the cell potentials with (V_{H_2+CO}) and without CO (V_{H_2}), that is, $E_{H_2+CO} = E_{H_2} + (V_{H_2} - V_{H_2+CO})$.

Cyclic voltammetry was carried out using the same single cell set-up, in the temperature range of 25–85°C. To investigate catalyst behavior with respect to the CO oxidation process, H_2 containing 100 ppm of CO was passed through the anode electrode for at least 1 h while maintaining a constant potential (0.05 V vs. RHE). At the same time pure hydrogen was passed through the cathode electrode which served as a RHE reference and counter electrode. After passing the CO mixed gas, the anode compartment was then purged with N_2 for about 30 min to remove residual H_2 gas and nonadsorbed CO. The cyclic voltammetric measurements were made in the potential range of 0.05–1.2 V vs. RHE for Pt/C and 0.05–0.7 V vs. RHE for PtRu/C and PtSn/C at a sweep rate of 20 mV/s.

3. Results and discussion

Fig. 1 presents the cell potential vs. current density characteristics at several temperatures for the fuel cell with a Pt/C anode supplied with H_2/CO[20 ppm]//O_2. In accordance with the profiles obtained in other experimental investigations [17–20], the presence of CO in the anode gas stream leads to a marked decrease of the fuel cell performance, which is more accentuated at

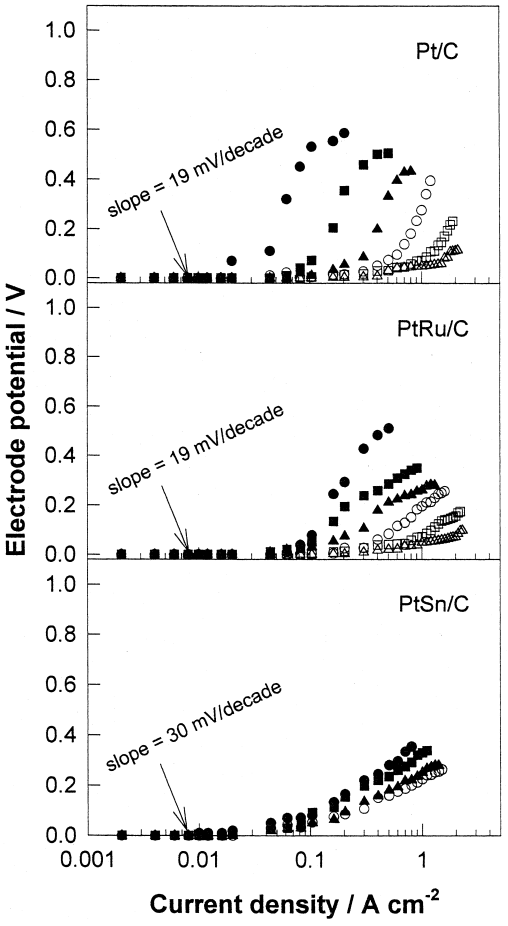

Fig. 4. Semilog plot of the polarization of hydrogen electrode for Pt/C, PtRu/C and PtSn/C with 20 ppm CO at several temperatures: (●) 40°C; (■) 55°C; (▲) 70°C; (○) 85°C; (□) 100°C and (△) 115°C corrected for ohmic losses.

the lower operating temperatures. Similar results were also obtained for systems with PtRu/C and PtSn/C anodes. The data obtained for these electrodes at several temperatures are presented in Fig. 2 and Fig. 3 in terms of the polarization responses of the hydrogen electrode as a function of current density in the absence, Fig. 2, and in the presence of 20 ppm of CO, Fig. 3. For comparison, the results obtained at each electrode in the presence of 20 ppm of CO at 55°C are also included in Fig. 2. The data for Pt/Sn above 85°C are not shown because this electrode was unstable at these temperatures, probably because of corrosion of the alloy. This instability in the PtSn/C performance was consistently observed above 85°C. The performance instability manifested in fluctuations in potential measurements, especially at higher current densities. Such fluctuations could be due to surface Sn dissolution at higher overpotentials (>600 mV) and instability of surface Sn oxy–hydroxide species at elevated temperatures. The exact mechanism remains unclear, however, the performance precludes its practical application as a viable PEM fuel cell anode electrocatalyst at temperatures above 85°C.

From the results in Fig. 2 it is evident that, in the range of current densities involved, the polarization of the hydrogen electrode in absence of CO is quite small and is not substantially affected by increase in temperature. On the other hand the results in Fig. 2 clearly show that the presence of CO, even in amount as low as 20 ppm, leads to a considerable increase in the electrode polarization, with the responses depending on the nature of the catalyst. This phenomenon is more clearly seen from the results of Fig. 3. For the Pt/C and Pt/Ru/C catalysts at lower temperatures there is a clear trend for the polarization response to reach a limiting current which persists over a temperature dependent range of overpotential, before converting to the more usual activation controlled exponential profile. The appearance of a limiting current is not clearly seen in the polarization diagram for PtSn/C which shows an exponential shaped profile for all temperatures in all regions of current density.

The differences in the polarization behavior in the presence of CO on the various catalysts may be attributed to the occurrence of different mechanisms for the CO poisoning effect. The analysis of these facts can be more appropriately made from the corresponding Tafel diagrams obtained by plotting the polarization data of Fig. 3 in a semilogarithm form. Fig. 4 shows these results for all catalysts. The Tafel diagrams can be analyzed taking into account the Tafel/Volmer mechanism for hydrogen oxidation reaction in acid media [15,21].

$$H_2 + 2S \longrightarrow 2S{-}H \quad \text{(Tafel) (I)}$$

$$S{-}H \longrightarrow S + H^+ + e \quad \text{(Volmer) (II)},$$

where S represents an active site in the catalyst surface.

In the absence of CO, the Tafel slopes are in the range of 20–30 mV dec^{-1} for all catalysts. According to the above mechanism, in absence of CO, both reactions (I) and (II) are very fast, corresponding to a very large exchange current density and a Tafel slope (b) close to 30 mV dec^{-1} [21]. On the other hand, in the presence of CO there is a large fraction of the surface covered with CO, meaning that reaction (I) may become the rate determining step. However, at a low reaction overpotential or low current densities the surface coverage of H may be enough to allow reaction (II) to occur at full speed which explains the value of Tafel slopes of 20–30 mV dec^{-1} obtained experimentally for overpotentials smaller than 50 mV Fig. 4. At

higher overpotentials, when reaction (I) becomes the rate determining step, the current generation is controlled by the rate of H adsorption, and a limiting current is observed in the polarization diagram. This corresponds to $b \rightarrow \infty$, as seen experimentally at intermediate overpotentials Fig. 4, especially for Pt/C and PtRu/C at temperatures below 85°C. According to the above model at high overpotentials the hydrogen current originates only from the oxidation of the S–H being formed on the holes of a compact CO surface monolayer [2,5,22].

In Fig. 4 it is seen that the magnitude of the limiting current depends on the temperature and on the nature of the catalyst. It is observed that the CO poisoning effect is smaller at higher temperatures and that, for temperatures below 85°C, the limiting current is higher in the sequence Pt/C < PtRu/C ≅ PtSn/C. Above 85°C the results indicate a similar poisoning effect for Pt/C and PtRu/C. Assuming no CO oxidation, it can be concluded that the bonding energy of CO with the catalyst surface atoms decreases with increase of temperature and is smaller for PtRu/C and PtSn/C compared to Pt/C. Above 85°C the CO bonding energy on Pt/C and PtRu/C becomes almost independent of the nature of the catalyst.

As mentioned above, the presence of a limiting current (i_L) is a consequence of the fact that reaction (I) is the rate determining step for the hydrogen oxidation in the presence of CO. In this case, from the kinetic treatment of reaction (I) it can be seen that the value of the limiting current will be proportional to the fraction of the surface (θ_s) free of adsorbed CO or H, that is,

$$i_L = k\theta_s^2, \quad (1)$$

where k is a rate constant, a term related to hydrogen pressure, the diffusion coefficient, and the Faraday law [17]. According to this equation the value of i_L increases with temperature because either k and/or θ_s increase with temperature. An increase in limiting current is evident from the plot representing the behavior of Pt/C in the temperature range of 40–70°C Fig. 3. At higher temperatures the classical limiting behavior is no longer observed, due to higher thermal motion causing creation of enough holes on the surface for reaction (I) to occur. In case of PtRu/C, the limiting behavior is observed only at low temperature (40°C) for 20 ppm of CO. The lack of limiting condition at temperatures lower than those observed for Pt/C is due to onset of CO oxidation brought about by the oxy–hydroxide species on alloyed ad-atoms Ru and Sn. Based on Arrhenius approach the current density i can be related to temperature using an expression:

$$\log i = \log C - \frac{2E_S}{2.303RT} - \frac{E_H}{2.303RT}, \quad (2)$$

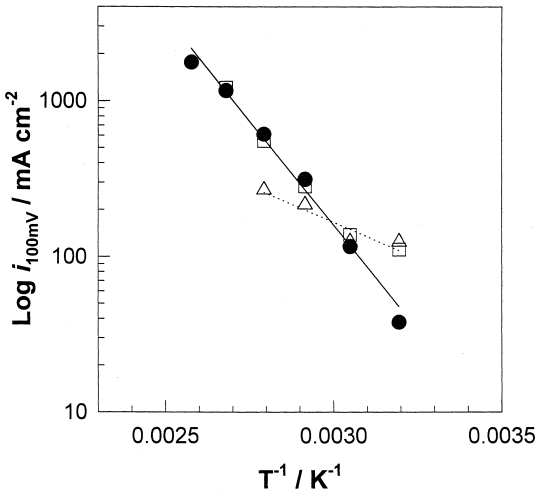

Fig. 5. Arrhenius plots for hydrogen oxidation on (●) Pt/C, (□) PtRu/C and (△) PtSn/C electrodes at 100 mV with 20 ppm CO.

where C is a constant containing terms related with the preexponential factor of the Arrhenius equation, the CO partial pressure, hydrogen partial pressure and the Faraday law. In Eq. (2) R and T have the usual meanings, E_H is the activation energy of reaction (I) and E_S is the activation energy of the process involved in the formation of free catalyst sites, which in the present conditions, is related with the desorption of CO.

Fig. 5 presents Arrhenius plots ($\log i$ vs. $1/T$) obtained for the three catalysts with H_2/CO[20 ppm]// O_2 at an electrode overpotential of 100 mV where it is assumed that kinetics is controlled by reaction (I). For Pt/C and PtSn/C straight lines covering the total range of temperature are obtained, which is good evidence for the validity of Eq. (2). From the slope of the lines in Fig. 5 it is calculated that ($2E_S + E_H$) is close to 51 kJ/mol for Pt/C and is 18 kJ/mol for PtSn/C. In the case of PtRu/C the slope changes with temperature, below 70°C it corresponds to that for PtSn/C while above this temperature it is close to that for Pt/C.

From the fact that the reaction kinetics in the absence of CO is essentially the same on all three catalysts, and assuming that the presence of CO does not affect the intrinsic catalytic property of the materials, it is concluded that E_H is independent of the catalyst material and is unaffected by the occurrence of reaction (I) either in the presence or in the absence of CO. Values for this parameter were obtained previously for Pt/C and several other catalysts including PtCr/C, PtMn/C, PtFe/C, PtCo/C, PtNi/C and the results are all very close to 11 kJ/mol [23]. If the same value is applied in the present case it is calculated that $E_S = 20$ kJ/mol for Pt/C and for PtRu/C ($T \geq 70$°C) and $E_S = 3.5$ kJ/mol for PtSn/C and for PtRu/C ($T \leq 55$°C).

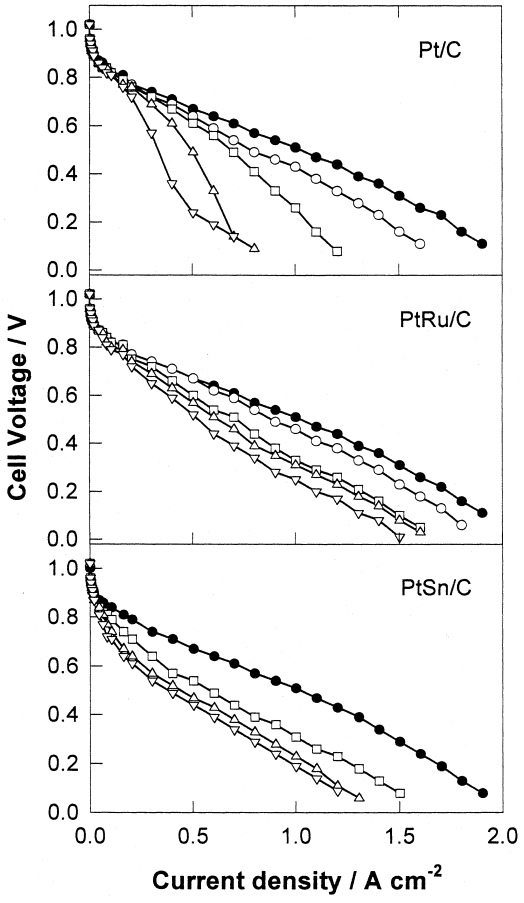

Fig. 6. Single Cell performance plots for Pt/C, PtRu/C and PtSn/C at 85°C at several CO concentrations: (●) 0 ppm; (○) 5 ppm; (□) 20 ppm; (△) 50 ppm and (▽) 100 ppm.

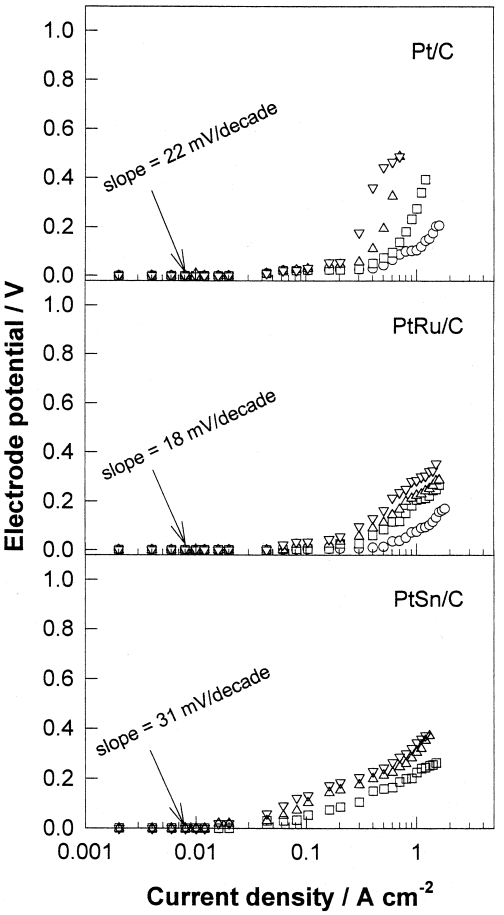

Fig. 7. Semilog plot of polarization of the hydrogen electrode for Pt/C, PtRu/C and PtSn/C at 85°C at several CO concentrations: (○) 5 ppm; (□) 20 ppm; (△) 50 ppm and (▽) 100 ppm, corrected for ohmic polarization losses.

Since E_s is related to oxidative desorption of CO, it reflects the strength and nature of CO bonding to the catalyst surface. Prior reports [10–14], have shown the possibilities of two distinctive bonding modes i.e. linear and bridge bonded CO species. The two distinct sets of values for E_s could be correlated to differences in CO bonding modes on Pt/C and PtRu/C ($T \geq 70$°C) and PtSn/C and PtRu/C ($T \leq 55$°C).

Fig. 6 and Fig. 7 present the effect of CO partial pressure on the performance of the fuel cell and on the polarization of the anode at a constant temperature (T = 85°C). In agreement with other work [17–19] the results in Fig. 6 show that the strongest effect of the CO partial pressure on the fuel cell performance occurs for the Pt/C catalyst. Although PtSn/C presents a higher CO tolerance than Pt/C at higher CO partial pressures, it shows much larger performance degradation at low partial pressure of 5 ppm of CO. The semilog plots of the hydrogen electrode polarization behavior Fig. 7 shows smaller values of limiting or quasilimiting currents (as the case may be) at higher CO partial pressures which is consistent with the degradation observed in fuel cell performance. Further, the values of Tafel slopes obtained at low current density are in the same range as those presented in Fig. 4 (20–30 mV dec^{-1}).

In an attempt to obtain the reaction order with respect to CO concentration, log–log plots of the limiting current obtained at 0.1 V as a function of CO concentration were plotted for the three catalysts (Fig. 8). The plots yielded reasonable straight lines and the corresponding slopes (reaction order) are −0.39 for Pt/C, −0.46 for PtRu/C and −0.88 for PtSn/C. These values can therefore be grouped into two sets, one for Pt/C and PtRu/C for which the reaction order is approximately $-\frac{1}{2}$ with respect to the CO concentration, and the other for PtSn/C where the reaction order is −1. Although it is very difficult to assign a

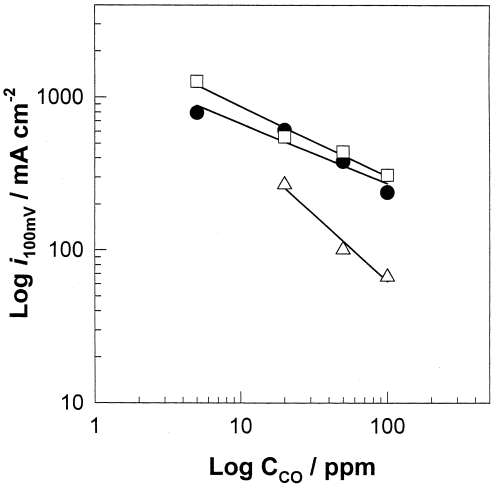

Fig. 8. Log–log plot of current density vs. CO concentration for hydrogen oxidation at 100 mV for (•) Pt/C, (□) PtRu/C and (△) PtSn/C electrodes at 85°C.

specific physical meaning for these reaction orders, these together with the activation energies are consistent with the presence of different types of adsorbed CO, that is bridge-bonded for Pt/C and PtRu/C and linear-bonded for PtSn/C.

Recent studies on smooth and high surface area electrodeposited Pt, PtRu and PtSn electrodes using in situ FTIR spectroscopy [23] at room temperature has shown the existence of both linear and bridge bonded CO on Pt. This agrees with previous results by Kunimatsu [24,25] and Iwasita et al. [26,27], using in situ FTIR (such as EMIRS, SNIFTIRS and SPAIRS) on smooth Pt electrodes at room temperature. Results on high surface area electrodeposited PtRu [23] at room temperature shows presence of linear bound CO species at low hydrogen overpotentials. These results are also supported by corresponding in situ FTIR-DRS spectroscopy [14] on unsupported Pt and PtRu (1:1) under conditions of methanol oxidation at room temperature. While the existence of both linear and bridge bonded CO was observed for Pt, PtRu showed existence of only linear bound CO. These room temperature infrared results agree with those from this investigation. However on the basis of the present results and their interpretation it is not possible to conclusively assign these different CO binding modes. This will be made in a forthcoming publication in which the reaction kinetics are modeled as a function of the CO partial pressure.

Important information about the behavior of the system was also obtained by recording the current decay at a constant cell potential as a function of time, after a pure hydrogen stream supplied to the anode was replaced by hydrogen containing CO. Fig. 9 presents the results of these studies which were conducted at a cell potential of 0.6 V for the three anode materials at several temperatures while maintaining the CO content at 20 ppm. Fig. 10 shows the results obtained at several CO concentrations while maintaining the temperature at 85°C, and Fig. 11 presents the results for a constant temperature (85°C) and CO concentration (20 ppm) but at different cell potentials.

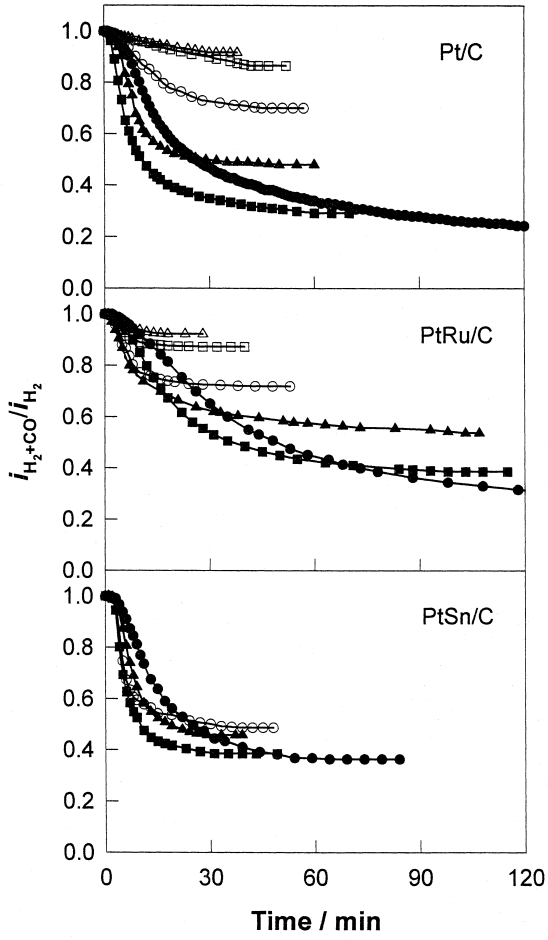

Fig. 9. i_{H_2+CO}/i_{H_2} vs. time at 0.6 V at several temperatures using 20 ppm CO: (•) 40°C; (■) 55°C; (▲) 70°C; (○) 85°C; (□) 100°C and (△) 115°C.

Fig. 9 shows the magnitude of the steady-state current ratio for Pt/C and PtRu/C is more affected by temperature than is the case for PtSn/C, which is consistent with the polarization curves. For Pt/C and PtRu/C a lowering of the CO partial pressure results in an increase of time required to reach the steady-state Fig. 10. For PtSn/C this time is approximately independent of pressure. Also in Fig. 10, it is observed that with 5 ppm CO there is a larger decrease of the current for PtSn/C than for Pt/C or PtRu/C. Finally from Fig. 11 it is observed that the extent of current

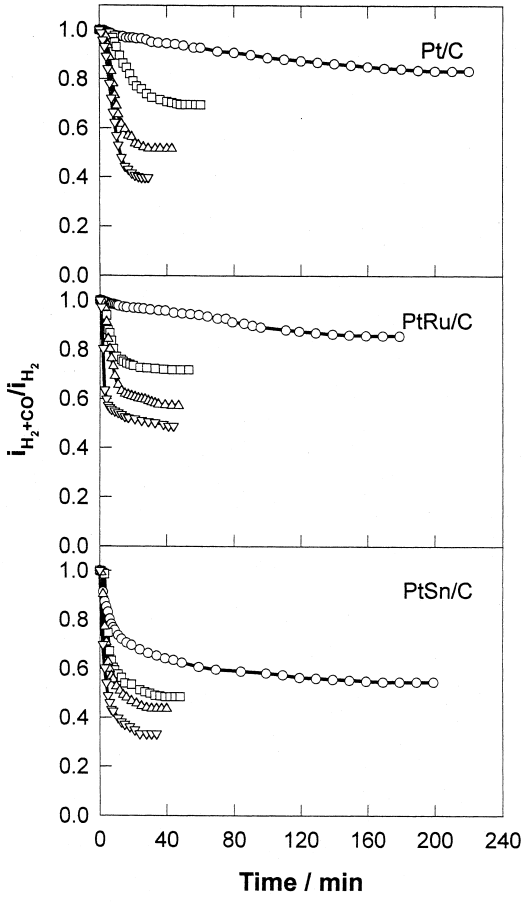

Fig. 10. i_{H_2+CO}/i_{H_2} vs. time for Pt/C, PtRu/C and PtSn/C electrodes at a cell potential of 0.6 V at 85°C for several CO concentrations: (○) 5 ppm; (□) 20 ppm; (△) 50 ppm and (▽) 100 ppm.

decay at 85°C with 20 ppm of CO is practically independent of potential (or current density) for PtSn/C, while this is not so for Pt/C or PtRu/C.

These common observations for Pt/C and PtRu/C in one hand, and for PtSn/C on the other, can be rationalized by assuming that the CO adsorption step depends on the catalyst nature and may occur through a replacement reaction or a free site attack, as proposed in other previously published reports [20]

$$2CO(g) + 2nS - -H \Leftrightarrow 2S_n - -CO + nH_2 \quad \text{replacement (III)}$$

$$CO(g) + nS \Leftrightarrow S_n - -CO \quad \text{free site attack (IV),}$$

where $n = 1$ for linear bonded CO and $n = 2$ for bridge bonded adsorbed CO. Some specific diagnostic criteria can be established to help in the assignment of one of these reactions to a given catalyst. Since reactions (I) and (II) are fast, it is concluded that in the initial condition of the time dependence experiments (absence of CO), the surface coverage by hydrogen does not change appreciably with current density hence the rate and the extension of reaction (III) is independent of the current density. On the other hand, the rate of formation of free sites (S) is obviously dependent on current density (see reaction II), indicating that the rate and the extension of reaction (IV) may be more affected by the value of current density.

In Figs. 9 and 11 it is seen that for PtSn/C the time required to reach the steady-state and the extent of current decay is less affected by temperature and is also practically independent of the cell potential. This indicates that for PtSn/C reaction (III) is the most probable route for the CO adsorption process. In the case of Pt/C and PtRu/C the dependence of the time vs. steady-state current ratio with the current density is

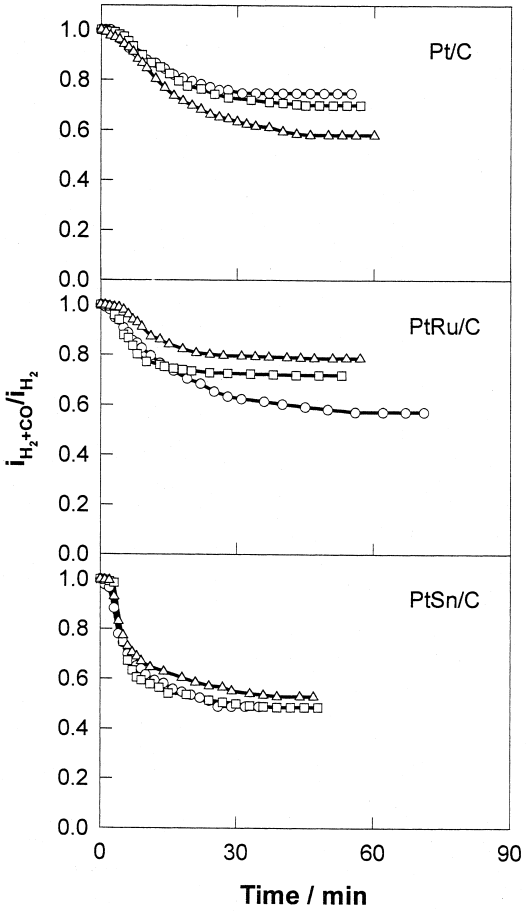

Fig. 11. i_{H_2+CO}/i_{H_2} vs. time for Pt/C, PtRu/C and PtSn/C electrodes at several cell potentials at 85°C using 20 ppm CO: (○) 0.8 V; (□) 0.6 V and (△) 0.4 V.

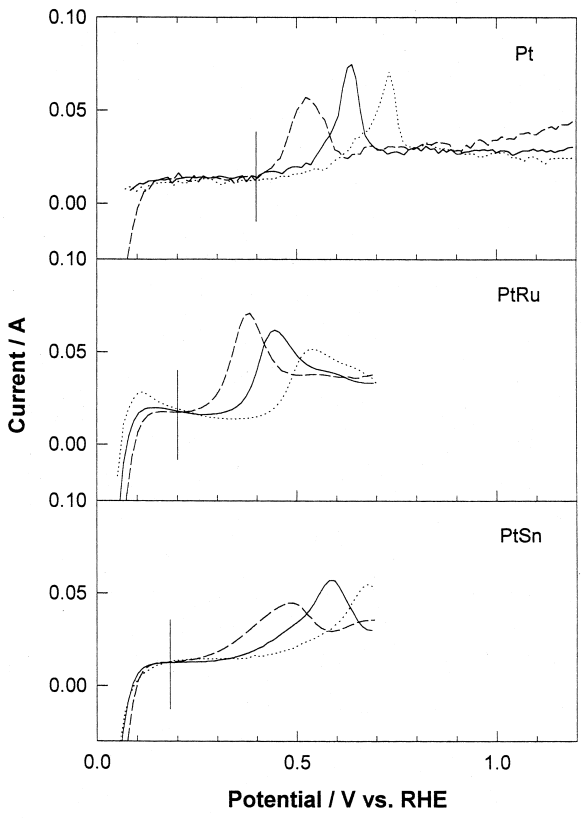

Fig. 12. Cyclic voltammograms for Pt/C, PtRu/C and PtSn/C electrodes with 100 ppm CO at several temperatures at a scan rate of 20 mV/s: (· · ·) 25°C; (———) 55°C and (- - -) 85°C.

much more indicative of participation of reaction (IV) (free sites).

Considering that reaction (IV) is operative for Pt/C and PtRu/C and reaction (III) for PtSn/C, several other observations can be made from the current vs. time profiles. In Fig. 9, it is shown that the rate of the CO poisoning effect is slower for PtRu/C followed by Pt/C and PtSn/C at all temperatures indicative of a slower overall rate of CO adsorption reaction for PtRu/C or Pt/C than for PtSn/C. Fig. 9 also shows that for Pt/C the time required to reach the steady-state, first decreases and then increases with the increase of temperature. For PtRu/C there is a continuous decrease of the time while for PtSn/C it decreases only up to 55°C. These results indicate that below 55°C in all cases the overall rate of reactions (III) or (IV) for all catalysts increases with temperature. Above this temperature the behavior becomes distinct for the various catalysts. In the case of Pt/C and PtRu/C it has to be noted that reaction (IV) competes with reaction (I) with respect to the occupation of the free catalyst sites generated by reaction (II). The rates of both reactions must increase with the temperature and, if the speed of reaction (I) becomes higher, there will be a relative decrease in the rate of reaction (IV) because of a diminution on the concentration of free sites. This seems to be the case for Pt/C. For PtRu/C the velocity of reaction (IV) must be always faster than that of reaction (I).

From the results in Figs. 4 and 7 it is observed that the limiting current is more evident for Pt/C than for either PtRu/C or PtSn/C. In the last two cases some increase of the current with overpotential is clearly observed in the region of the plateau. In Fig. 11, the CO poisoning effect decreases with the decrease of cell potential or equivalently with the increase of hydrogen electrode potential especially for PtRu/C and PtSn/C. This behavior can be analyzed in terms of the occurrence of the CO oxidation reaction as proposed previously [17–20]

$$S--H_2O + S--CO \longrightarrow S + CO_2 + 2H^+ + 2e \quad (V).$$

The extent of CO oxidation is dependent on the temperature, the cell potential, and the nature of the catalyst. The occurrence of this reaction leads to the opening of free catalyst sites (S) for hydrogen adsorption and, as a consequence, to an increase of the H coverage which will lead to an increase of the current for hydrogen oxidation, eventually preventing the establishment of a limiting currents in Figs. 3 and 4 or Fig. 7.

Fig. 12 shows the anodic portions of the cyclic voltammograms corresponding to the CO oxidation process as a function of temperature for the Pt/C, PtRu/C and PtSn/C. It is observed that for all catalysts the CO oxidation process is shifted to lower electrode potentials with increase in temperature. At a constant temperature, the onset of CO oxidation occurs at lower electrode potential in the sequence PtSn/C < PtRu/C < Pt/C, as indicated by the vertical lines drawn in Fig. 12 for $T = 85$°C. However, it is observed that the peak potential does not follow the same sequence with PtSn/C and PtRu/C swapping places. An examination of the i vs. E profiles for all temperatures clearly indicates that this behavior is a consequence of the fact that the CO oxidation process has slower electrochemical kinetics on PtSn than on either Pt/C or PtRu/C.

Another important point to be learned from the results in Fig. 12 is that even at 85°C the onset of the CO oxidation process for PtSn/C or PtRu/C only occurs above potential of ca. 0.2 V. However, comparison of the polarization data in Fig. 3, shows that at lower temperatures PtRu/C has a higher CO tolerance even for potentials below 0.1 V. Since in both PtRu/C and Pt/C, the CO adsorption step is the same, that is reaction (IV), this behavior indicates that the CO tolerance is not only related to the onset of the CO oxi-

dation step but it also depends on the nature of the CO bonding to the catalyst surface. This fact is confirmed from an examination in the hydrogen desorption region of the voltammograms of Fig. 12. It is seen that for Pt/C the hydrogen adsorption/desorption process appears blocked at all temperatures while for PtRu/C a clear trend of a trade-off between CO and hydrogen adsorption is seen at lower temperature.

Some of the above conclusions are applicable to PtSn/C but in this case the comparison is more difficult because the CO adsorption step occurs through a different path. In any case the increased CO tolerance is due to oxygenated species (oxy–hydroxides of Sn) at lower overpotentials compared to Pt/C as confirmed from the results on Figs. 3, 4 and 7. Also, the slower kinetics for CO oxidation explain why the increase in the hydrogen oxidation current due to the onset of CO oxidation is not as pronounced for PtSn/C as for the other catalysts.

4. Conclusions

In this work the kinetics of the hydrogen oxidation reaction on Pt/C, PtRu/C, and PtSn/C electrocatalysts in the presence of CO was analyzed taking into account the several steps for the CO poisoning mechanism. It is proposed that the CO adsorption step occurs predominantly through a displacement path (reaction III) for PtSn/C and through a free site attack path (reaction IV) for Pt/C and PtRu/C. The data strongly points towards different types of absorbed CO, linear or bridge bonded on the three electrocatalysts.

It is observed that the onset of CO oxidation process occurs at different potentials depending on the nature of the electrode material. Independently of temperature, the onset of this reaction occurs first for PtSn/C followed by PtRu/C and finally for Pt/C. Occurrence of reaction (V) explains very satisfactorily many of the CO tolerance factors for the alloy catalysts, although very important, it is not the only factor responsible for the CO tolerance effect. Other contributors are the changes promoted by the alloyed materials on the thermodynamics and the kinetics of the CO adsorption process.

Acknowledgements

The authors acknowledge the support of the US Department of Energy under Contract No. DE-AC02-98CH10886. S.J.L. was supported by a 1996 Abroad Post-Doc. Program from Ministry of Education, Korea. E.A.T. is on leave of absence from Instituto de Quimica de Sao Carlos/USP, Brazil, with a scholarship from Fundacao de Amparo a Pesquisa do Estado de Sao Paulo (FAPESP).

References

[1] H.A. Gasteiger, N. Markovic, P.N. Ross Jr., E.J. Cairns, J. Phys. Chem. 98 (1994) 617.
[2] H.A. Gasteiger, N.M. Markovic, P.N. Ross Jr., J. Phys. Chem. 99 (1995) 8290.
[3] H.A. Gasteiger, N.M. Markovic, P.N. Ross Jr., J. Phys. Chem. 99 (1995) 16757.
[4] K. Wang, H.A. Gasteiger, N.M. Markovic, P.N. Ross Jr., Electrochim. Acta 41 (1996) 2587.
[5] B.N. Grgur, G. Zhuang, N.M. Markovic, P.N. Ross Jr., J. Phys. Chem. 101 (1997) 3910.
[6] W.T. Napporn, J.-M. Leger, C. Lamy, J. Electroanal. Chem. 408 (1996) 141.
[7] K.L. Ley, R. Liu, C. Pu, Q. Fan, N. Leyarovska, C. Segree, E.S. Smotkin, J. Electrochem. Soc. 144 (1997) 1543.
[8] K.Y. Chen, P.K. Shen, A.C.C. Tseung, J. Electrochem. Soc. 142 (1995) L185.
[9] K.Y. Chen, A.C.C. Tseung, J. Electrochem. Soc. 143 (1996) 2703.
[10] J. Sobkowski, A. Czerwinski, J. Phys. Chem. 89 (1985) 365.
[11] B. Beden, C. Lamy, N.R. de Tacconi, J. Arvia, Electrochim. Acta 35 (1990) 691.
[12] M. Hachkar, T. Napporn, J.-M. Léger, B. Beden, C. Lamy, Electrochim. Acta 41 (1996) 2721.
[13] H. Igarashi, T. Fujino, M. Watanabe, J. Electroanal. Chem. 391 (1995) 119.
[14] Q. Fan, C. Pu, E.S. Smotkin, J. Electrochem. Soc. 143 (1996) 3053.
[15] W. Vogel, J. Lundquist, P. Ross, P. Stonehart, Electrochim. Acta 20 (1975) 79.
[16] H.P. Dhar, L.G. Christner, A.K. Kush, H.C. Maru, J. Electrochem. Soc. 133 (1986) 1574.
[17] T.A. Zawodzinski Jr., C. Karuppaiah, F. Uribe, S. Gottesfeld, in: J. McBreen, S. Mukerjee, S. Srinivasan (Eds.), Electrode Materials and Processes for Energy Conversion and Storage IV, vol. 97–13, The Electrochemical Society Inc, 1997, pp. 15–24.
[18] H.-F. Oetjen, V.M. Schmidt, U. Stimming, F. Trila, J. Electrochem. Soc. 143 (1996) 3836.
[19] T. Springer, T. Zawodzinski, S. Gottesfeld, in: J. McBreen, S. Mukerjee, S. Srinivasan (Eds.), Electrode Materials and Processes for Energy Conversion and Storage IV, vol. 97–13, The Electrochemical Society Inc, 1997, pp. 139–146.
[20] R.J. Bellows, E.P. Marucchi-Soos, D. Terence Buckley, Ind. Eng. Chem. Res. 35 (1996) 1235.
[21] R.M.Q. Mello, E.A. Ticianelli, Electrochim. Acta 42 (1997) 1031.
[22] A. Couto, M.C. Pérez, A. Rincón, C. Gutiérrez, J. Phys. Chem. 100 (1996) 19538.
[23] Y. Morimoto, E.B. Yeager, J. Electroanal. Chem. 441 (1998) 77.

[24] K. Kunimatsu, H. Seki, W.R. Golden, J.G. Gordon II, M.R. Philpott, Langmuir 2 (1985) 596.
[25] K. Kunimatsu, K. Shimazu, H. Kita, J. Electroanal. Chem. 256 (1988) 371.
[26] T. Iwasita, F.C. Nart, J. Electroanal. Chem. 317 (1991) 291.
[27] T. Iwasita, F.C. Nart, B. Lopez, W. Vielstich, Electrochim. Acta. 37 (1992) 2361.